Opsin 3 is a key regulator of ultraviolet A-induced photoageing in human dermal fibroblast cells*

Y. Lan, Y. Wang and H. Lu

Department of Dermatology, Affiliated Hospital of Guizhou Medical University, Guiyang, Guizhou 550001, China

Summary

Correspondence
Hongguang Lu.
E-mails: hongguanglu@hotmail.com;
luhongguang@gmc.edu.cn

Background Chronic exposure to ultraviolet (UV) radiation (mainly UVA) induces a sustained increase of matrix metalloproteinases (MMPs), especially MMP1, MMP2, MMP3 and MMP9 in human skin fibroblasts. MMPs can lead to the degradation of fibrous connective tissue, which is the main cause of skin photoageing. The molecular mechanisms through which fibroblasts sense UVA and trigger the cell signalling pathways involved in the upregulation of MMPs have not been well elucidated.

Objectives Here, we investigated the function and potential mechanisms of photoageing of opsin (OPN)3 in normal human dermal fibroblasts (NHDFs).

Methods Real-time polymerase chain reaction and Western blot analysis were used to analyse the expression levels of OPN3 in NHDFs and photoageing models. Subsequently, NHDFs transfected with OPN3 inhibitors and indicators related to photoageing before and after UVA irradiation included expression levels of MMP1, MMP2, MMP3 and MMP9, and signalling pathway protein molecules were examined.

Results We provide evidence that OPN3 initiates UVA phototransduction in NHDFs. OPN3 triggers phosphorylation of activator protein 1 and ultimately upregulates MMP1, MMP2, MMP3 and MMP9 in NHDFs through activating Ca^{2+}/calmodulin-dependent protein kinase II, cyclic adenosine monophosphate response element-binding protein, extracellular signal-regulated kinase, c-JUN N-terminal kinase and p38. Here, we demonstrate for the first time that OPN3 is the key sensor responsible for upregulating MMP1, MMP2, MMP3 and MMP9 in NHDFs following UVA exposure via the calcium-dependent G protein-coupled signalling pathway.

Conclusions Our studies provide insights into the understanding of the molecular mechanisms through which human skin cells respond to UVA radiation and may reveal molecular targets for skin photoageing prevention or clinical management.

What's already known about this topic?

- Photoaged fibroblasts accumulate with long-term ultraviolet (UV) exposure.
- Matrix metalloproteinases (MMPs) play an important role in the pathogenesis of photoageing.
- MMP1, MMP2, MMP3 and MMP9 are responsible for the destruction of fibroblast collagen in severely photodamaged skin.
- Opsins (OPNs) are light-sensitive members of the superfamily of heptahelical G protein-coupled receptors, a family of cell surface receptors that are activated by a variety of stimuli and mediate signalling across membranes.

What does this study add?

- OPN3 is highly expressed in fibroblasts and responds to UVA irradiation.

- OPN3 regulates the expression of MMP1, MMP2, MMP3 and MMP9 via the calcium-dependent G protein-coupled signalling pathway.
- OPN3 is a light-sensitive sensor that plays an important role in photoageing of the skin.

As the primary barrier from the effects of the external environment, human skin is regularly exposed to ultraviolet (UV) radiation.[1] Prolonged or excessive UVA radiation induces skin photoageing.[2] A wealth of evidence has indicated that the induction of matrix metalloproteinases (MMPs) plays an important role in the pathogenesis of photoageing, and MMP1, MMP2, MMP3 and MMP9 are the major collagenolytic enzymes that are responsible for the destruction of fibroblast collagen in severely photodamaged skin.[3–6] However, the key mechanisms of fibroblasts that sense and respond to UVA irradiation in human skin have not been fully elucidated.

Opsins (OPNs) belong to the photosensitive G protein-coupled receptor (GPCR) superfamily, which mediate phototransduction through the GPCR signalling pathway.[7–13] The human OPNs family is divided into five subfamilies including OPN1 (cone opsins), OPN2 (rhodopsin), OPN3 (encephalopsin, tmt-opsin), OPN4 (melanopsin) and OPN5 (neuropsins). The visual OPNs[7] include OPN1 and OPN2, while the nonvisual OPN subfamily contains OPN3, OPN4 and OPN5.[11] Light absorption and G-protein activation are the two main functions of most OPN subfamilies. In the human retina, OPN2 underlies twilight vision, while OPN1 plays a role in daylight vision.[11,14] Recent studies have demonstrated that OPNs also exist in the extraocular tissues including skin.[15–18] OPN2 plays critical roles in the regulation of the melanogenesis of melanocytes.[19] OPN3 is a nonvisual OPN highly expressed in skin, and yet its function remains unknown.[16] Our previous studies have shown that OPN3 upregulates the activity of tyrosinase in human epidermis melanocytes, cocultured with keratinocytes *in vitro*,[17] and OPN3 might be responsible for hyperpigmentation induced by visible light.[20] Another study suggests that knockdown of OPN3 led to a reduction in early differentiation of keratinocytes following irradiation with blue light.[21] In the brains of zooplankton, OPN3 can sense UV-activated intracellular signalling cascades.[22] In mice, OPN4 was responsible for the vasodilatation response to blue light.[23] OPN5 acts as a UV-sensitive photoreceptor to activate Gi-mediated light transduction pathways in humans and mice.[24] Visible light [or UV radiation (UVR)] consists of photons, which can activate OPN GPCRs that elicit cellular responses through activation of different G proteins and downstream effectors.[8,13,22,25,26] However, whether OPNs can also act as photoreceptors in human fibroblasts is still unclear.

In this study, we have observed that UVA irradiation upregulates MMP1, MMP2, MMP3 and MMP9 in human skin fibroblasts through OPN3. UVA irradiation, OPN3 triggers phosphorylation of activator protein 1 via the calcium-dependent G protein-coupled signalling pathway and ultimately upregulates MMP1, MMP2, MMP3 and MMP9 in human skin fibroblasts through activating Ca^{2+}/calmodulin-dependent protein kinase (CAMK)II, cyclic adenosine monophosphate response element-binding (CREB) protein, extracellular signal-regulated kinase (ERK), c-JUN N-terminal kinase (JNK) and p38. Our study provides insights into the understanding of the molecular mechanisms through which human skin cells respond to UVA radiation and may reveal molecular targets for skin photoageing prevention or clinical management.

## Materials and methods

Cell culture

Normal human dermal fibroblasts (NHDFs) were surgically derived from the foreskin of paediatric patients aged 3–12 years (Affiliated Hospital of Guizhou Medical University, Guiyang, China). Cells were cultured in dishes containing Dulbecco's modified Eagle's medium (DMEM) (11965092, Gibco, Gaithersburg, MD, U.S.A.) supplemented with 10% fetal bovine serum (FBS) (10100147, Gibco), penicillin (100 U mL^{-1}) and streptomycin (100 mg mL^{-1}). Cells were cultured at 37 °C in a humidified incubator (Forma, Thermo Fisher Scientific, Waltham, MA, U.S.A.) with 5% CO_2 and used at their seventh passage when the cells were actively proliferating. The research protocol was reviewed and approved by the ethics committee of the Affiliated Hospital of Guizhou Medical University.

Ultraviolet A irradiation

Solar UV Simulator SUV-1000 (Sigma, Shanghai, China) with an emission spectrum between 320 nm and 400 nm served as the UVA source. UVA dose was measured using a UVA radiometer (Sigma, Shanghai, China). Prior to UVA irradiation, NHDFs were washed twice with phosphate-buffered saline (PBS) and cultured in PBS to avoid the side-effects associated with photosensitization in the culture medium. For the inhibition experiments, NHDFs were preincubated for 5 min with 9 μmol L^{-1} U73122 (S8011, Selleck Chemicals, Houston, TX, U.S.A.) and were then irradiated with UVA at 10 J cm^{-2}. The cell lysates were collected for further research 48 h after UVA irradiation.

Cell viability tests

Cell viability was determined using Cell Counting Kit (CCK)-8 Cell Proliferation and Cytotoxicity Assay Kit (CA1210, Solarbio
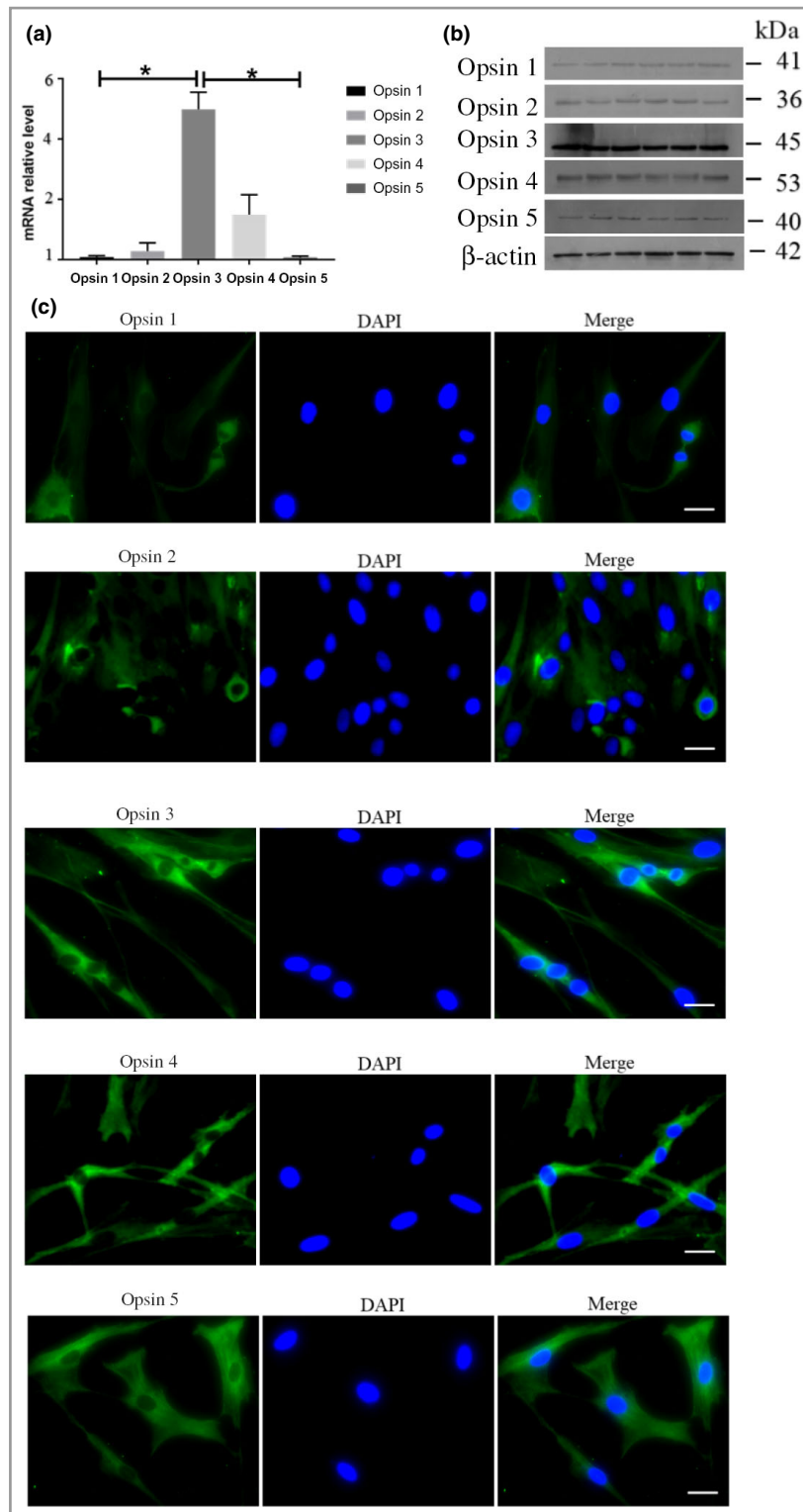
Fig 1. Opsins were expressed in normal human dermal fibroblasts (NHDFs). (a) Reverse transcription quantitative polymerase chain reaction analysis of human opsin transcript expression. Opsin mRNA levels were normalized with glyceraldehyde 3-phosphate dehydrogenase levels (n = 3 independent experiments). *$P < 0.05$. (b) Western blot analysis of opsin protein expression in NHDFs. (c) Representative images show opsin protein expression (using previously published opsin antibodies) in NHDFs. The left panel represents the localization of opsins (green) at the plasma membrane, the middle panel represents the nucleus stained with 4′,6-diamidino-2-phenylindole (DAPI) (blue) and the right panel represents an overlay of the middle panel and the phase contrast image. Scale bars = 20 μm (n = 3 independent experiments).
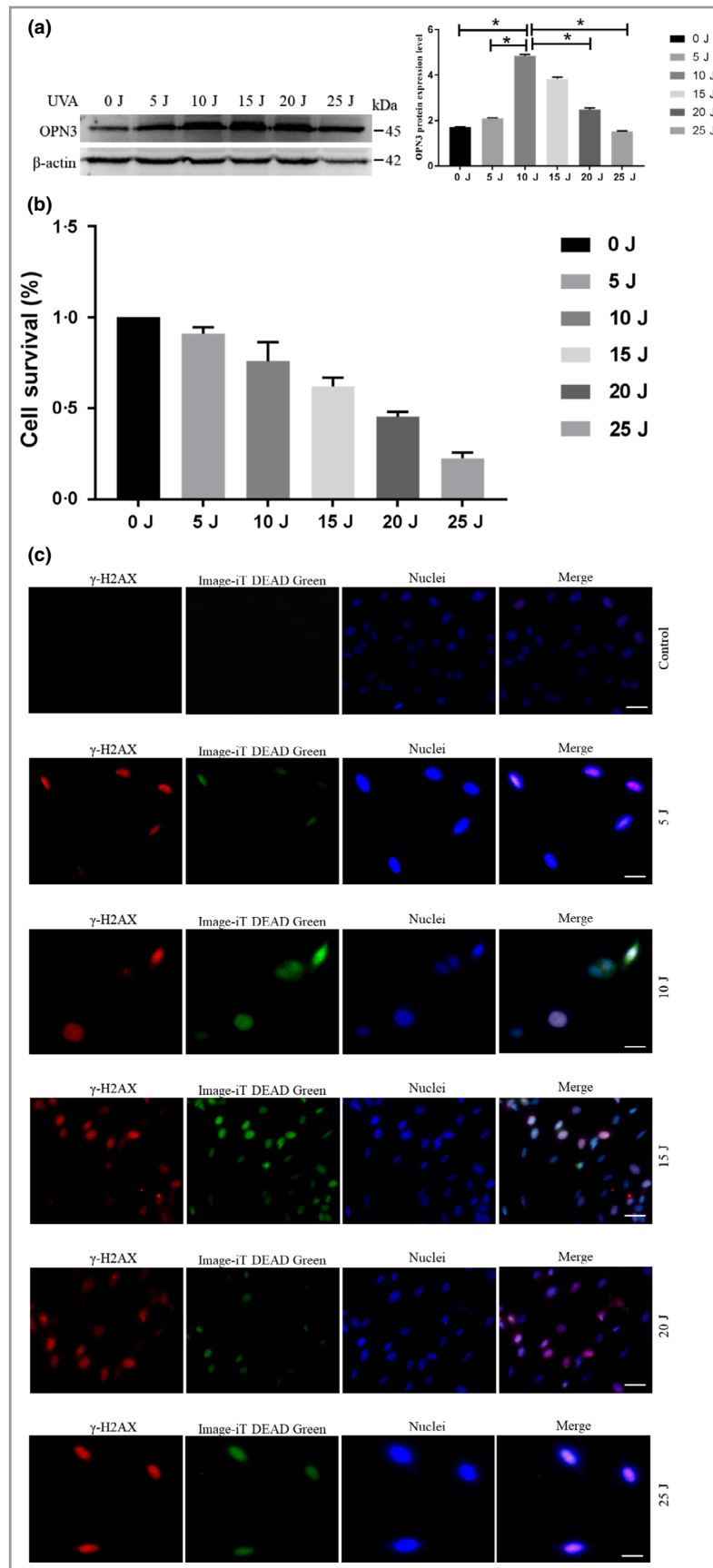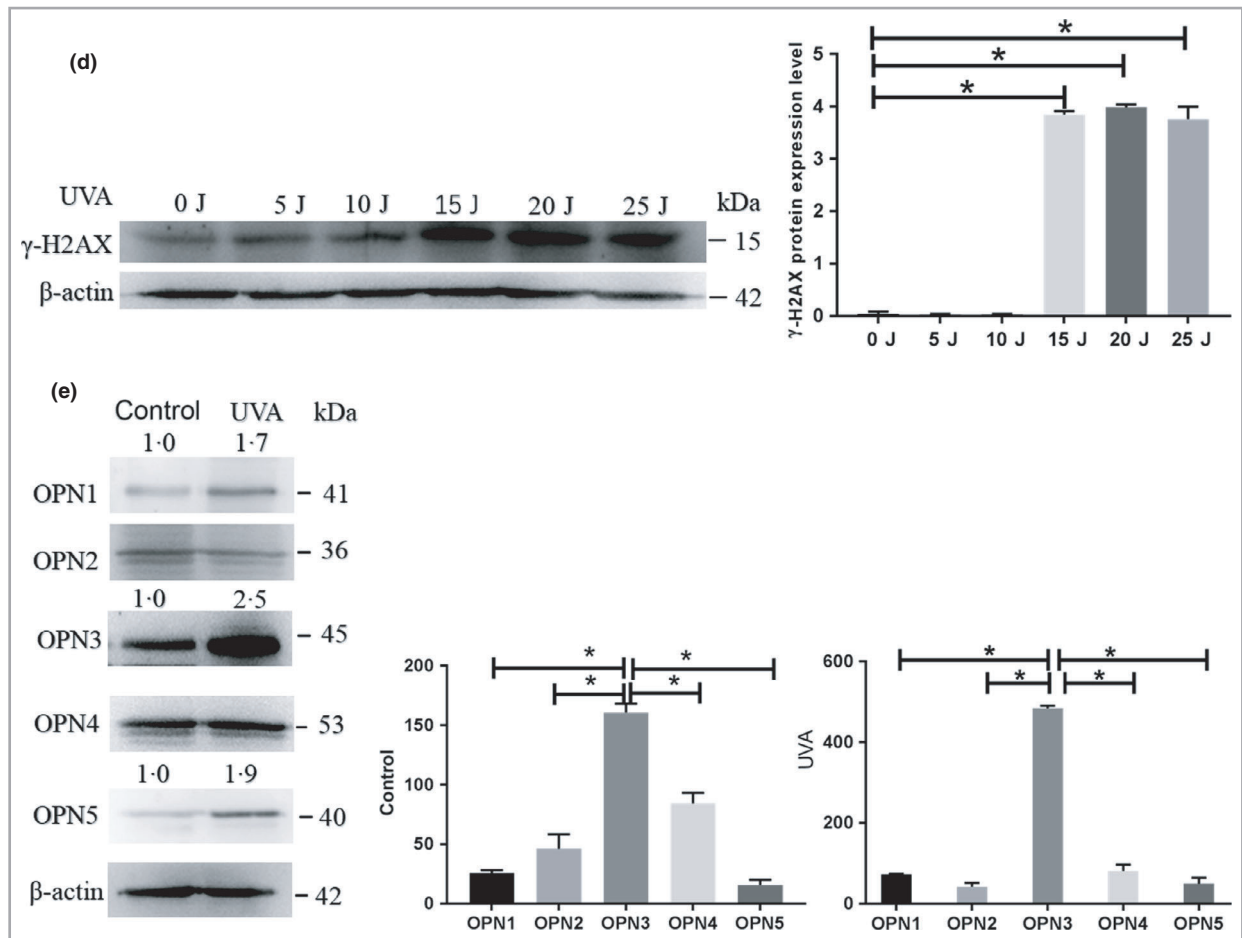
Fig 2. Continued.

Fig 2. Ultraviolet (UV)A irradiation induces opsin (OPN)3 expression in normal human dermal fibroblasts. (a) Relative OPN3 protein expression level was shown after exposure to UVA radiation (0 J cm^{-2}, 5 J cm^{-2}, 10 J cm^{-2}, 15 J cm^{-2}, 20 J cm^{-2}, 25 J cm^{-2}). (b) Fibroblasts were irradiated with UVA and cell viability was measured 48 h later. (c) DNA damage with/without UVA-irradiated fibroblasts was assessed using light microscopy. Nuclei were stained using Hoechst 33342 and indicated as blue. Cell membranes were stained by Image-iT DEAD Green and shown as green. Scale bars = 20 μm. (d) Phosphorylated H2AX was analysed by immunoblotting 48 h after irradiation of fibroblasts with different doses of UVA. (e) Fibroblasts were irradiated with UVA (10 J cm^{-2}), and the expression level of OPN protein was determined using Western blot analysis. Western blot analyses were normalized using actin as a loading control and the relative protein level was quantified using Quantity One software (n = 3 independent experiments). In all panels, data are shown as the mean ± SEM of the indicated number of independent experiments. Statistical significance was determined by one-way analysis of variance (ANOVA) followed by Tukey's test. *P < 0·05.

Life Sciences, Beijing, China). In brief, NHDFs were incubated overnight in 96-well culture plates at a concentration of 1 × 10^4 cells per well. When 60% confluence was reached, cells were treated with UVA irradiation. Following 24 h of incubation, 10 μL CCK-8 solution was added and incubated at 37 °C for an additional 2 h. The absorbance at 450 nm was then measured, and the cell viability was expressed as the percentage of the absolute optical density of each sample relative to that of the control value.

RNA extraction and quantitative real-time reverse transcription quantitative polymerase chain reaction

Total RNA was isolated using TRIzol (Invitrogen, Carlsbad, CA, U.S.A.), and reverse transcription was performed with 2·5 μg total RNAs using cDNA Synthesis kit (Invitrogen, U.S.A.). Quantitative real-time TaqMan reverse transcription quantitative polymerase chain reaction (RT-PCR) technology (7500Fast, Applied Biosystems, Foster City, CA, U.S.A.) was used to determine the expression levels of the selected target genes. Levels of target genes were calculated using the $2^{-\Delta\Delta Ct}$ method and determined as the fold increase over the expression in controls. The following human primers (Generay Biotech Co. Ltd, Shanghai, China) were used in this study: opsin1-sw F, 5′-TGTGCCTCTCTCCCTCATCT-3′; opsin1-sw R, 5′-GGCACGTAGCAGACACAGAA-3′; OPN2 F, 5′-GAGTCAGCC ACCACACAGAA-3′; OPN2 R, 5′-CATGAAGATGGGACCGAAG TTGGAG-3′; OPN3 F, 5′-CAATCCAGTGATTTATGTCTTCATGA TCAGAAAG-3′; OPN3 R, 5′-GCATTTCACTTCCAGCTGCTGGTA GGT-3′; OPN4 F, 5′-TCCTCCTCTTCGTGCTCT 3′; OPN4 R,

5′-GTAAATGATGGGGTTGTGG 3′; OPN5 F, 5′-CTAGACGAAA GAAGAAGCTGAGACC-3′; OPN5 R, 5′-GCGGTGACAAAAGCAA GAGA-3′; GAPDH F, 5′-GACATCCGCAAAGACCTG-3′; GAPDH R, 5′-GGAAGGTGGACAGCGAG-3′.

Western blot analysis

Cells were harvested and total protein concentrations were measured using Pierce® BCA Protein Assay Kit (23227, Thermo Fisher Scientific). After heat denaturation, 40 µg of proteins were subjected to sodium dodecyl sulfate–polyacrylamide gel electrophoresis and then transferred onto polyvinylidene difluoride membranes. The membrane was blocked with 5% skimmed milk in tris-buffered saline with Tween 20 for 2 h at room temperature and then incubated with primary antiopsin antibody (Medical Discovery Leader), including anti-OPN1 (MD11128-100), anti-OPN2 (MD11129-100), anti-OPN3 (MD4034-100), anti-OPN4 (MD4194-100), anti-OPN5 (MD4195-100); anti-MMP1 (MD672-050), anti-MMP3 (MD722-100), anti-CERB (MD1367), anti-p38 (MD6295-100), anti-c-fos (MD6452-20), anti-phospho-c-Jun (ser73) (MD1278-20), anti-c-Jun (MD679-20), anti-JNK (MD1929-20), anti-phospho-JNK (MD1483-20), anti-MMP9 (MD5640-100), anti-MMP2 (GTX104577, GeneTex, Irvine, CA, U.S.A.), anti-Histone H2A.XS139ph (phospho Ser139) (GTX127340, GeneTex), anti-tissue inhibitor of metalloproteinase (TIMP)1 (ab109125, Abcam, Cambridge, U.K.) and β-actin mouse monoclonal antibody (MD409-100, Medical Discovery Leader). After washing, the membrane was incubated with secondary antibody (MD912527, Medical Discovery Leader) for 1 h at room temperature. Specific bands were visualized using a chemiluminescent reaction (electrogenerated chemiluminescence; E003-50, 7 Sea Biotech, Shanghai, China). Band intensity was quantified with Quantity One software (BioRad, Hercules, CA, U.S.A.). All values were normalized to the corresponding β-actin results.

Immunofluorescence

For immunostaining, cells were inoculated on coverslips at a density of 4×10^4 cells for 24 h and were washed three times with PBS. The cells were fixed with 95% ethanol at room temperature for 10 min and then dried at room temperature. Blocking was performed with 10% normal goat serum (Invitrogen) in PBS-T for 30 min. For staining, cells were incubated with antibodies (1 : 50, Medical Discovery Leader), including anti-OPN1 (MD6494-100), anti-OPN2 (MD6495-

100), anti-OPN3 (MD6496-100), anti-OPN4 (MD6497-100), anti-OPN5 (MD6498-100), anti-MMP1 (MD672-100), anti-MMP3 (MD88-100), anti-MMP9 (MD683-100), anti-MMP2 (ab86607, Abcam) and anti-Histone H2A.XS139ph (phospho Ser139) (GTX127340, GeneTex) overnight at 4 °C, followed by incubation with fluorescent labelled secondary antibodies (Medical Discovery Leader) for 1 h. Cells were mounted and visualized under a confocal microscope (Carl Zeiss, Oberkochen, Germany).
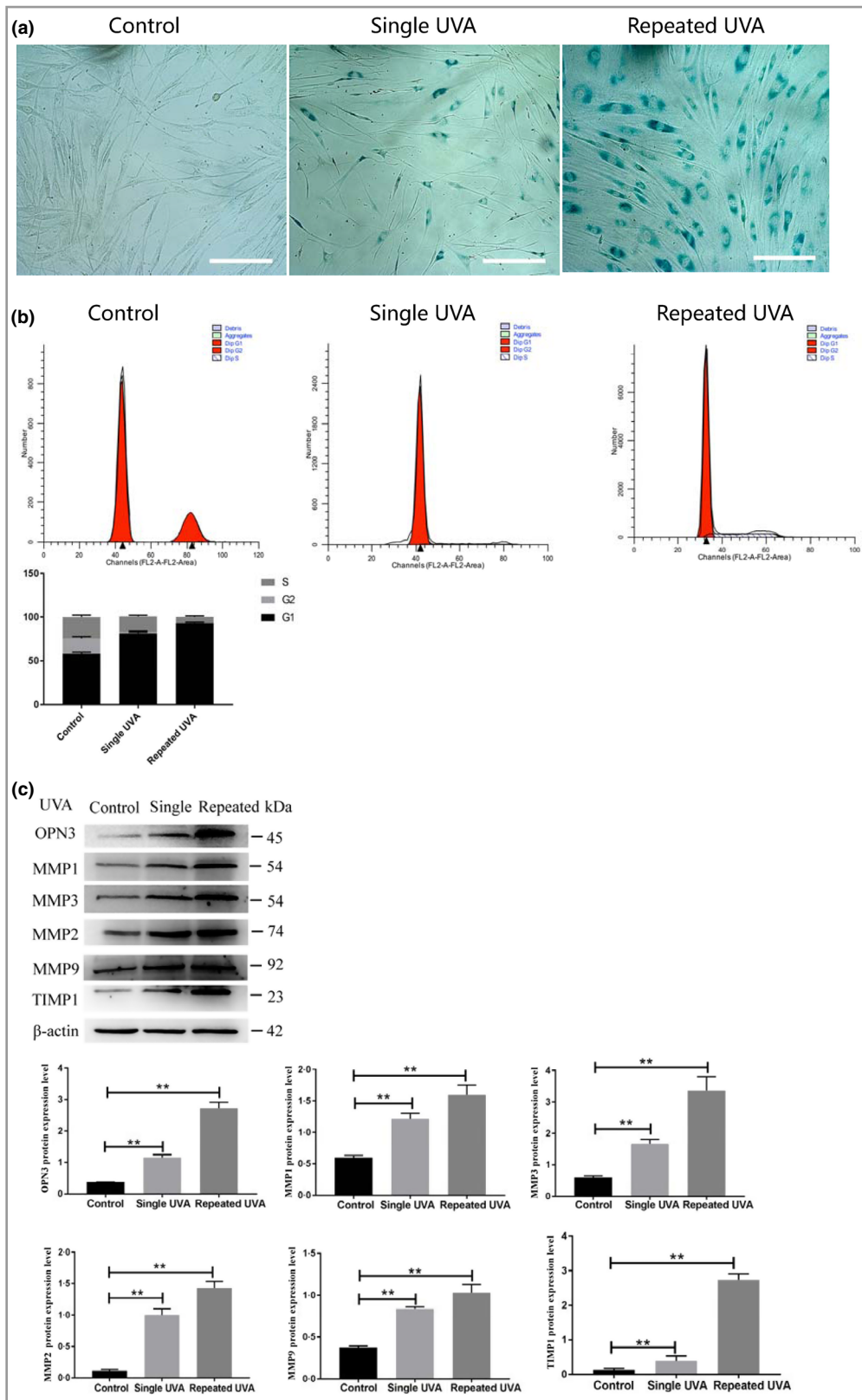
Laser scanning microscopy for DNA damage stain

NHDFs were plated in 35-mm round glass-bottom dishes overnight in a 5% CO_2 atmosphere at 37 °C using DMEM. The cells were irradiated with different doses of UVA and then cultured for an additional 48 h under normal cell culture conditions. To test cell viability, Image-iTDEAD Green (Thermo Fisher Scientific) was added to the cells and allowed to incubate for 30 min under normal cell culture conditions. The cells were then fixed in a 4% paraformaldehyde solution for 15 min, permeabilized by a Triton X-100 solution (15 µL in 6 mL PBS) for 15 min and blocked by a bovine serum albumin (BSA) solution (0·25g in 25 mL PBS) for 1 h. Subsequently, a solution of the primary antibody pH2ax was added to the cells and incubated for 1 h. The Alexa Fluor 555 conjugated secondary antibody/Hoechst 33342 nuclear counterstain (CA1120, Solarbio) (3 µL/1µL in 6 mL BSA blocking buffer) was added to the cells and incubated for an additional 1 h. Finally, the cells were washed with PBS buffer and imaged by microscopy.

Knockdown of opsin 3

Small interfering (si)RNA transfection was performed using OPN3 siRNA mix (ARD-2, Viewsolid Biotech, Beijing, China) targeting OPN3 protein and control siRNA (ARD-1, Viewsolid Biotech). The silence efficiency of the siRNA-OPN3 sequences was analysed 48 h post-transfection via quantitative RT-PCR and compared with negative control siRNAs that did not target any known gene. The siRNA sequence with the strongest silence efficiency on OPN3 was used for the follow-up study and levels of OPN3 gene silencing were assessed 24 h, 48 h and 72 h post-transfection by qPCR. We selected 48 h as the time point for observation in the later experiment. NHDFs were transfected using RNAiMAX (TranSheepBio-Tech Co.

Fig 3. Overexpression of opsin (OPN)3 in the cell model for photoageing of normal human dermal fibroblasts following repeated UVA exposure. (a) Cells were stained with a β-galactosidase staining kit. Blue colour indicates senescent cells. Scale bars = 50 µm. (b) G1 arrest was analysed in untreated control cells or UVA-irradiated cells using flow cytometry on day 14. (c) Cultured cells were untreated or irradiated for 14 days and collected to detect OPN3, matrix metalloproteinase (MMP)1, MMP2, MMP3, tissue inhibitors of metalloproteinases (TIMP)1 and MMP9 using Western blot analysis. β-actin was used as a loading control. The relative protein level was quantified using Quantity One software ($n = 3$ independent experiments). In all panels, data are shown as the mean ± SEM of the indicated number of independent experiments. One-way analysis of variance (ANOVA) followed by Tukey's test was used unless otherwise indicated. **$P < 0.01$.

(a)

Control Single UVA Repeated UVA

(b)

Control Single UVA Repeated UVA

(c)

© The Authors. *British Journal of Dermatology*
published by John Wiley & Sons Ltd on behalf of British Association of Dermatologists.

Ltd., Shanghai, China) according to the manufacturer's protocol in a final concentration of 50 nmol L^{-1}. After transfection of NHDFs for 48 h, the transfection efficiency was analysed using Western blot and qPCR.

Calcium imaging and calcium flux analysis

Fluo-3/AM was used to monitor changes in intracellular Ca^{2+} concentration. NHDFs were plated on six-well plate at density of 4×10^4. After UVA irradiation, cells were washed with 1 mL of serum-free DMEM and loaded with 2·5 μmol L^{-1} Fluo-3/AM [#S1056, MultiSciences (Lianke) Biotech Co. Ltd., Hangzhou, China] in serum-free DMEM for 30 min at 37 °C in the darkroom. Afterwards, cells were washed with 1 mL of serum-free DMEM, and fluorescent images of Fluo-3/AM-loaded cells were acquired using Cell Observer-Living Cells (Carl Zeiss).

In addition, cells were also harvested and incubated with 1 mL serum-free DMEM containing 2·5 μmol L^{-1} Fluo-3/AM for 30 min at 37 °C in the darkroom. Fluo-3/AM-loaded NHDFs were centrifuged at 1000 **g** for 5 min at room temperature, washed once with 0·1 mol L^{-1} PBS buffer solution and resuspended with 0·5 mL of 0·1 mol L^{-1} PBS buffer solution. Then the concentration of intracellular free calcium ion was measured with Fluo-3/AM flow cytometric assay (BD Biosciences, San Jose, CA, U.S.A.). The excitation source for Fluo-3/AM was a 488-nm air-cooled argon laser and the emission was measured using a 525-nm band pass filter.

Statistical analysis

All experiments were performed independently at least three times. All values were expressed as mean ± SD. Statistical significance was determined by a one-way analysis of variance (ANOVA). P values < 0·05 were considered statistically significant.

Results

Overexpression of opsin 3 in normal human dermal fibroblasts

To demonstrate the expression of OPNs in NHDFs, the mRNA and protein level of OPNs were detected using qPCR and Western blot analysis, respectively. Our results showed that OPN1,

OPN2, OPN3, OPN4 and OPN5 are expressed in NHDFs (Fig. 1a, b) and immunofluorescence results showed that OPNs stained positively in NHDFs (Fig. 1c). Interestingly, the expression of OPN3 in the mRNA and protein level is significantly higher than other OPNs (Fig. 1a, b), suggesting that OPN3 may play an important functional role in NHDFs.

Ultraviolet A induces expression of opsin 3 in a dose-dependent manner in normal human dermal fibroblasts

OPN3 can sense UV to activate intracellular signalling cascades and it can directly bind exogenous all-*trans*-retinal.[22] Mosquito OPN3 activates Gαi/o subunits of G proteins in a light-dependent manner and the Gβγ subunits that dissociate from Gαi could activate phospholipase C (PLC)-β and cause a Ca^{2+} response.[27] Therefore, we reasoned that OPN3 may be the GPCR that mediates UVR phototransduction in NHDFs. To determine whether OPN3 mediates UVR phototransduction, we studied the protein expression of OPN3 in NHDFs using different single doses ranging from 5 J cm^{-2} to 25 J cm^{-2} of UVA exposure according to a previous report.[28] Our results showed that UVA increases the expression of OPN3 in a dose-dependent manner. The expression of OPN3 increases at a dose of 5 J cm^{-2}, reaches a peak at 10 J cm^{-2} and then declines gradually (Fig. 2a), indicating that OPN3 responds to UVA.

Next, we tested cell viability using the CCK-8 assay following a single 10 J cm^{-2} UVA exposure in accordance with previous reports.[29] As shown in Figure 2b, 48 h after UVA irradiation, more than 75% of cells remained viable. DNA damage is the predominant deleterious effect of UVR on cells. In mammalian cells, damage to genomic DNA can be lethal, inducing the formation of phosphorylated H2AX.[30] In our study, DNA damage was detected using a red fluorescent antibody against phosphorylated H2AX. At the same time, cell viability was investigated by Image-iT DEAD Green, which permeates when the plasma membrane is compromised. The results show that NHDFs affected by UVA radiation exhibited dramatically increased DNA damage (red) and cell death (green) (Fig. 2c). Moreover, Western blot analysis showed a significant increase in phosphorylated H2AX protein levels at ≥ 15 J cm^{-2}, suggesting more severe DNA damage. Furthermore, phosphorylated H2AX protein levels were not statistically significant at 5 J cm^{-2} and 10 J cm^{-2} compared with the control group (Fig. 2d). Therefore, in

Fig 4. Ultraviolet (UV)A upregulates the expression of matrix metalloproteinase (MMP)1, MMP2, MMP3 and MMP9 via opsin (OPN)3. (a) OPN3 colocalized with MMPs (MMP1, MMP2, MMP3 and MMP9) in normal human dermal fibroblasts (NHDFs) with immunofluorescence double-staining method. Expression localization of OPN3 (green) and MMPs (red) with or without UVA irradiation is depicted. The fluorescence intensity of the recorded NHDF increased in response to UVA. Scale bars = 20 μm. (b) NHDFs were transfected with small interfering (si)RNA directed against OPN3 or control. The efficiency of siRNA was determined by Western blot analysis. (c) The efficiency of siRNA was determined by quantitative polymerase chain reaction (n = 3 independent experiments). (d, e) Cells were transfected with siRNA against OPN3 irradiated with or without 10 J cm^{-2} UVA and lysed after 48 h. Lysates were analysed by Western blot using the indicated antibodies. In all panels, data are shown as the mean ± SEM of the indicated number of independent experiments. One-way analysis of variance (ANOVA) followed by Tukey's test was used. *P < 0·05 and **P < 0·01. Blots are representative of three or more independent experiments.

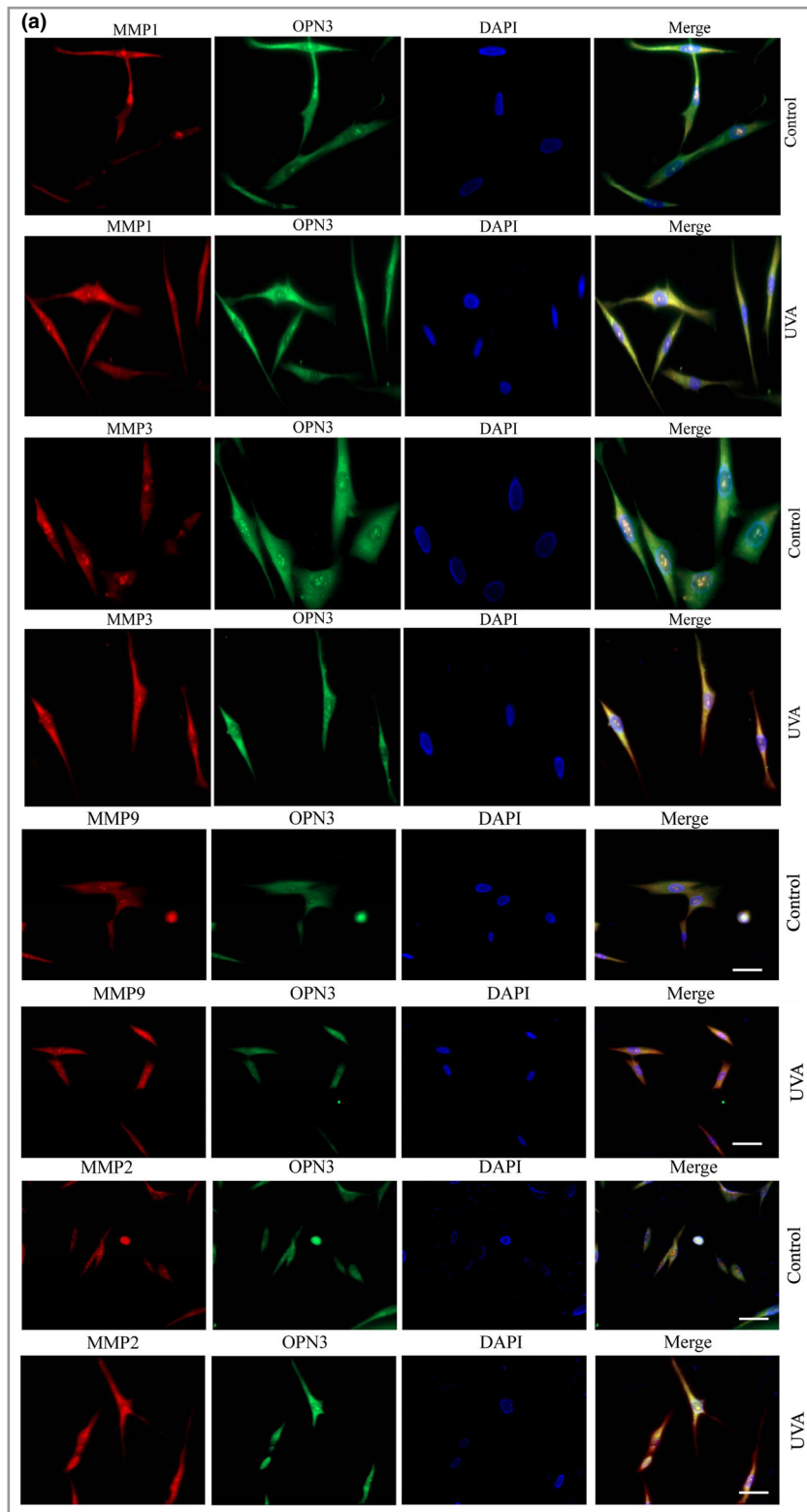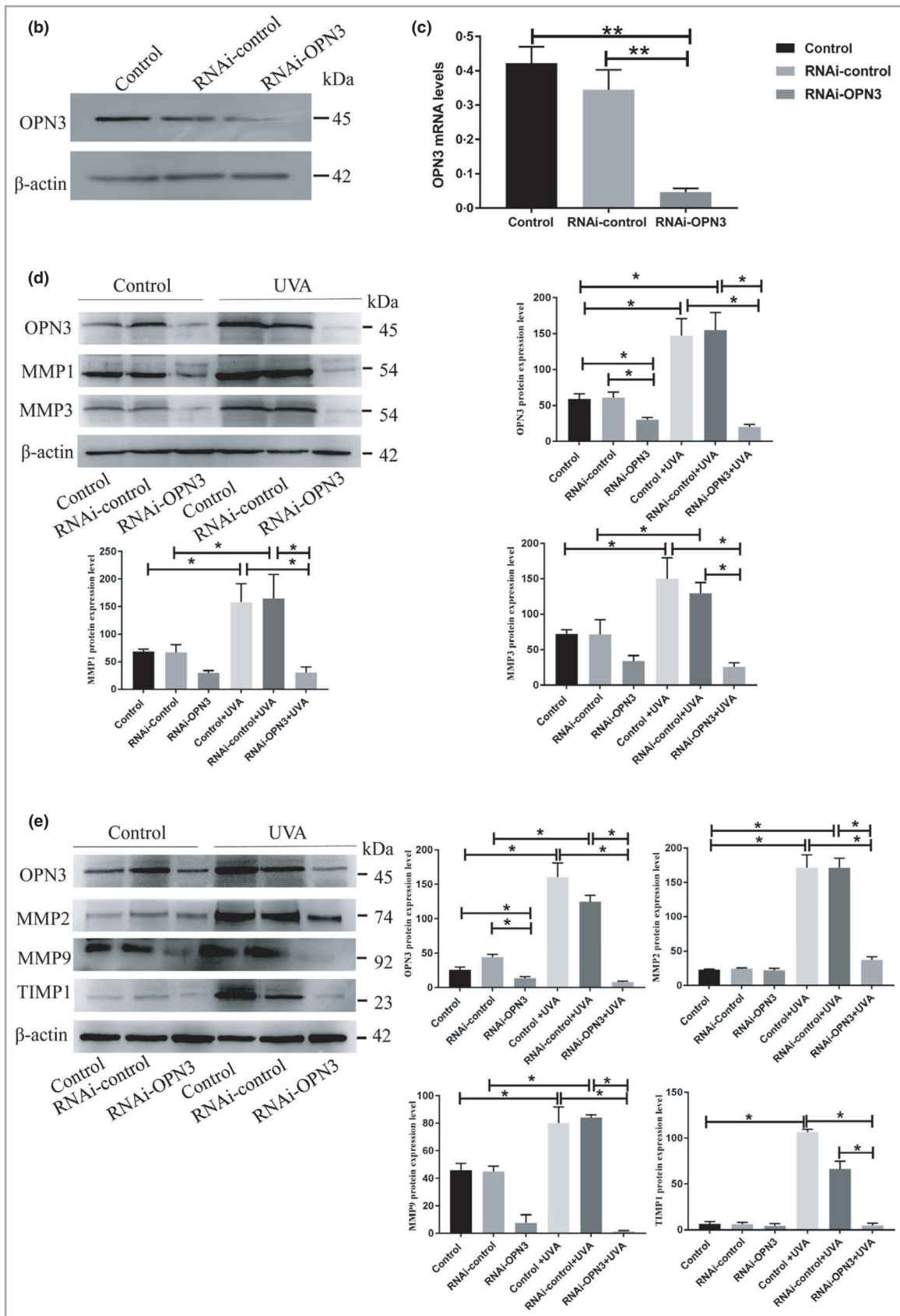**Fig 4.** Continued.

conjunction with previous experimental research methods,[29] 10 J cm^{-2} UVA was used in the following experiments for subsequent studies.

Additionally, after irradiating the cells with 10 J cm^{-2} UVA, we examined the expression of five OPNs. Our results further showed that the expression of OPN3 (irradiation group, 2·5-fold increase) was significantly higher than that of OPN1 (irradiation group, 1·7-fold increase) and OPN5 (irradiation group, 1·5-fold increase). OPN2 and OPN4 expression did not change significantly (Fig. 2e).

Overexpression of opsin 3 in the cell model for normal human dermal fibroblast photoageing following repeated 10 J cm⁻² ultraviolet A exposure

Previous studies have demonstrated that repeated 10 J cm^{-2} UVA irradiation of fibroblasts results in photoageing.[29] In this study, we established a model for NHDF photoageing following repeated 10 J cm^{-2} UVA exposure for 14 days *in vitro*. Cells were analysed after 14 consecutive daily UVA irradiations with senescence-associated β-galactosidase (β-gal) staining[31–33] and flow cytometry, respectively.[34] The staining results of β-gal showed that the percentage of β-gal-positive cells was significantly increased by UVA irradiation at day 14 (Fig. 3a). Cells in the control group and UVA-irradiated group were further subjected to G1 arrest test by flow cytometry[34] and the results in Figure 3b showed that the percentage of UVA-irradiated cells in the G1 phase was higher than control cells, suggesting that UVA elicits a G1 arrest in cultured fibroblasts. Therefore, photoageing was successfully induced in fibroblasts using repeated 10 J cm^{-2} UVA exposure *in vitro*. At the same time, we found that the expression of OPN3, MMP1, MMP2, MMP3 and MMP9 also increased after 14 days of consecutive UVA irradiation (Fig. 3c). Moreover, the expression of TIMP1, a negative regulator of MMP activity, was also significantly increased (Fig. 3c), which was consistent with previous studies.[34]

Ultraviolet A upregulates the expression of matrix metalloproteinases 1, 2, 3 and 9 via opsin 3

We further demonstrated that OPN3 and MMP1, MMP2, MMP3 and MMP9 were coexpressed in NHDFs using immunofluorescence staining (Fig. 4a). After knockdown of OPN3 in the mRNA and protein level (Fig. 4b, c) using siRNA that targeted the OPN3 gene, NHDFs were irradiated with 10 J cm^{-2} UVA. No significant changes were observed in the expression of MMP1, MMP2, MMP3, TIMP1 and MMP9 protein 48 h later (Fig. 4d, e). These results indicated that UVA upregulates the expression of MMP1, MMP2, MMP3, MMP9 and TIMP1 in fibroblasts via OPN3.

Opsin 3 regulates the expression of matrix metalloproteinases 1, 2, 3 and 9 via the calcium-dependent G protein-coupled signalling pathway

Previous research has demonstrated that activation of GPCRs leads to an increase of calcium flux.[19,20] To determine whether UVA induces calcium flux in fibroblasts, we measured the intracellular calcium level in NHDFs with Fluo-3/AM probes following UVA irradiation. Intracellular calcium rose to a higher level in NHDFs after UVA exposure (Fig. 5a, b), and UVA induced the upregulation of pCAMKII (Fig. 5c), which is a key enzyme in the calcium pathway.[20] In addition to the calcium pathway activation, UVA also induces the phosphorylation of transcription factor CREB protein (Fig. 5c). CREB is a primary downstream target of CAMKII.[35–37] Then, we measured the UVA-induced response in NHDFs for knockdown of OPN3 with siRNA and found that preincubation significantly reduced Ca^{2+} response (Fig. 5d) and that the protein level of pCAMKII and pCREB was not changed (Fig. 5e). The UVA-induced Ca^{2+} response was affected by the absence of OPN3 expression.

As mosquito OPN3 activates Gαi/o subunits of G proteins in a light-dependent manner, and the Gβγ subunits that dissociate from Gαi could activate PLC-β and cause a Ca^{2+} response,[27] we blocked PLC-β with 9 μmol^{-1} U73122, which is essential for the calcium pathway. Results indicated that treatment of fibroblasts with U73122 significantly inhibited Ca^{2+} transients (Fig. 5f) and decreased expression of MMP1, MMP2, MMP3 and MMP9 (Fig. 5g). Furthermore, treatment of fibroblasts with U73122 significantly inhibited UVA-induced Ca^{2+} transients (Fig. 5h), and there was no change in the expression of MMP1, MMP2, MMP3 and MMP9 (Fig. 5i). These results further bolster our conclusion that OPN3 mediates calcium-dependent phototransduction of UVA in fibroblasts.

In addition, UVA also induces mitogen-activated protein kinase (MAPK) (p38, JNK and ERK) signalling pathways and downstream phosphorylation of target proteins c-fos and c-jun, as they are involved in the expression of MMPs (Fig. 5j). We further demonstrated that the downregulation of OPN3 in NHDFs with siRNA blocked the calcium flux induced by UVA and inhibited phosphorylation of ERK, JNK, p38, c-fos and c-jun (Fig. 5k). These data further suggest that OPN3 is a key sensor for UVA signalling in NHDFs.

Taken together, we conclude that in NHDFs, UVA activates OPN3 receptors leading to increased calcium flux. In response to calcium, CAMKII is phosphorylated and further induces phosphorylation of CREB, p38, JNK and ERK, and finally upregulates expression of MMP1, MMP2, MMP3 and MMP9 (Fig. 5l).

Discussion

OPN is a photosensitive receptor protein belonging to the GPCR superfamily, which plays a crucial role in visual sensitivity, circadian rhythm and pupillary light reflex in the human retina.[7,38–40] Previous studies have indicated that OPNs also exist in the extraocular tissues including skin.[19,25,41] Recently, OPN1-SW, OPN2, OPN3 and OPN5, which can sense visible light and UVR in the skin, have been reported to be expressed in keratinocytes and melanocytes.[19,20,42] Another recent article

reported that OPN receptors (OPN1-SW, OPN3 and OPN5) were similarly localized in the epidermis of human facial and abdominal skin in situ.[21] Furthermore, both mRNA and protein expression of OPN1-SW and OPN3 were confirmed in the papillary fibroblasts of healthy women.[21] Interestingly, OPN2, OPN4 and OPN5 were not detected in dermal fibroblasts in cell cultures. We have also previously confirmed that OPN (OPN1-SW, OPN2, OPN3, OPN4 and OPN5) is expressed in dermal fibroblasts from human foreskin.[43] The differences in the expression of OPN proteins may be due to differences in anatomical location or sex.

OPN proteins covalently bind to a vitamin A-based retinaldehyde chromophore through a Schiff base linkage to a lysine residue in the seventh transmembrane alpha helix. In vertebrates, the chromophore is either 11-cis-retinal (A1) or 11-cis-3,4-didehydroretinal (A2) and is found in the retinal binding pocket of the OPN. The absorption of a photon of light results in the photoisomerization of the chromophore from the 11-cis to an all-trans conformation. The photoisomerization induces a conformational change in the OPN protein, causing the activation of the phototransduction cascade. Different OPNs (or different classes of OPNs in different species) have different absorption spectra. OPN1 and OPN2, which mediate daylight (colour) and twilight vision in the human eye, have been reported in human epidermis, suggesting a potential light-sensitive role in the skin.[21] Interestingly, we have observed the presence of OPN1 in human dermal fibroblasts that were activated by blue light (420–440 nm),[21] which does not penetrate far into dermal skin. However, OPN1 may respond to UVR at 420 nm, as the UVR wavelength ranges from 280 nm to 420 nm. Human OPN5 and mouse OPN5 have maximum absorption peaks at 380 nm. In our study, UVA (320–40 nm; 10 J cm^{-2}) induced OPN1 and OPN5 expression. OPN2 and OPN4 do not respond to UVA, as the absorption spectra of OPN2 (with an absorption peak at a longer wavelength of 505 nm) and OPN4 (with an absorption

peak at a longer wavelength of 480 nm) are not in the UV range. However, a recent study showed that in normal Melan-a melanocytes and in malignant B16-F10 cells, UVA radiation increases the expression of OPN4 and melanin content.[44]

Furthermore, in our study, UVA radiation increased the expression of OPN3 and MMPs. OPN3 is a GPCR with a wide range of distribution, which includes the eyes, brain, testes, liver and kidneys.[7,26,45–47] As OPN3 homologs are expressed in tissues that are not considered photosensitive, it will be important to determine whether they form photopigments. Results from the research by Koyanagi et al. showed that PufTMTOPN3 and MosOPN3 have peak absorbance at 465 nm and 500 nm, respectively.[47] These results suggest that tissues expressing OPN3 homologs may be photosensitive. Recent reports have confirmed that OPN3 is the key sensor in melanocytes responsible for hyperpigmentation induced by blue light.[20] Blue light has also been shown to stimulate hair follicle growth via OPN3.[45] Another article suggests that an increase in OPN3 expression in the epithelial skin of the tongue may be a potential mechanism for the stimulation of wound closure by blue light.[21] Interestingly, some recent studies indicated that OPN3 does not mediate calcium-dependent phototransduction of UVR, blue light or green light in melanocytes and that OPN3 is a negative regulator of melanin levels in human melanocytes.[27] In summary, it is currently controversial whether OPN3 acts as a photoreceptor.

The expression of OPN3 was recently found in the ciliary photoreceptor cells of the annelid *Platynereis dumerilii* and was termed c(iliary)-opsin.[48] This c-opsin is UV-sensitive (λ_{max} = 383 nm) and can be tuned by 125 nm at a single amino acid (range λ_{max} = 377–502nm), demonstrating the ability of c-opsin to transmit UV signals to intracellular signalling cascades and that it can directly bind exogenous all-trans-retinal.[22] Mutational analyses revealed that a single amino-acid residue, Lys-94, underlies the two molecular properties.[22] In our study, we demonstrated that UVA induces expression of OPN3

Fig 5. Matrix metalloproteinase (MMP) expression induced by ultraviolet (UV)A and opsin (OPN)3 stimulation is calcium dependent. (a) Images of representative normal human dermal fibroblasts (NHDFs) loaded with the Ca^{2+} indicator Fluo-3 and stimulated with 10 J cm^{-2} UVA (n = 3 independent experiments). The fluorescence intensity of the recorded NHDFs increased in response to UVA. Scale bar = 20 μm. (b) UVA irradiation of fibroblasts and calcium flux is quantified using Fluo-3/AM. Red traces represent control group, blue traces represent the experimental group. (c) Phosphorylated Ca^{2+}/calmodulin-dependent protein kinase (CaMK)II and cyclic adenosine monophosphate response element-binding (CREB) protein were analysed by immunoblotting 48 h after irradiation of fibroblasts with different doses of UVA. (d, e) NHDFs transfected with siRNA directed against OPN3 or control were stimulated with UVA (10 J cm^{-2}). Calcium flux was quantified with Fluo3/AM. Red traces represent control groups, blue traces represent RNAi-control group, green traces represent RNAi-OPN3 group and protein lysate was analysed by Western blot. (f, g) NHDFs treated with U73122 (9 μmol L^{-1}). Calcium flux was quantified with Fluo3/AM (red traces represent control groups and blue traces represent experimental group) and protein lysate was analysed by Western blot. (h, i) NHDFs treated with U73122 (9 μmol L^{-1}) were stimulated with 10 J cm^{-2} UVA, calcium flux was quantified with Fluo3/AM (red traces represent control group, blue traces represent U73122 group, green traces represent UVA irradiation group and protein lysate was analysed by Western blot). (j) Fibroblasts were irradiated with and without UVA (10 J cm^{-2}), and the expression level of protein was determined by Western blot analysis. (k) Cells were transfected with siRNA against OPN3 irradiated with 10 J cm^{-2} UVA and lysed after 48 h. Lysates were analysed by Western blot using the indicated antibodies. Blots are representative of three or more independent experiments. (l) Summary model of the key findings in this study. OPN3 is the key sensor responsible for upregulating the expression of MMP1, MMP2, MMP3 and MMP9 in fibroblasts following UVA exposure via the calcium-dependent G protein-coupled signalling pathway. In all panels, data are shown as the mean ± SEM of the indicated number of independent experiments. One-way ANOVA followed by Tukey's test was used. *P < 0·05 and **P < 0·01. TRP, transient receptor potential, JNK, c-JUN N-terminal kinase; ERK, extracellular signal-regulated kinase; AP-1, activator protein 1; PLC phospholipase C.
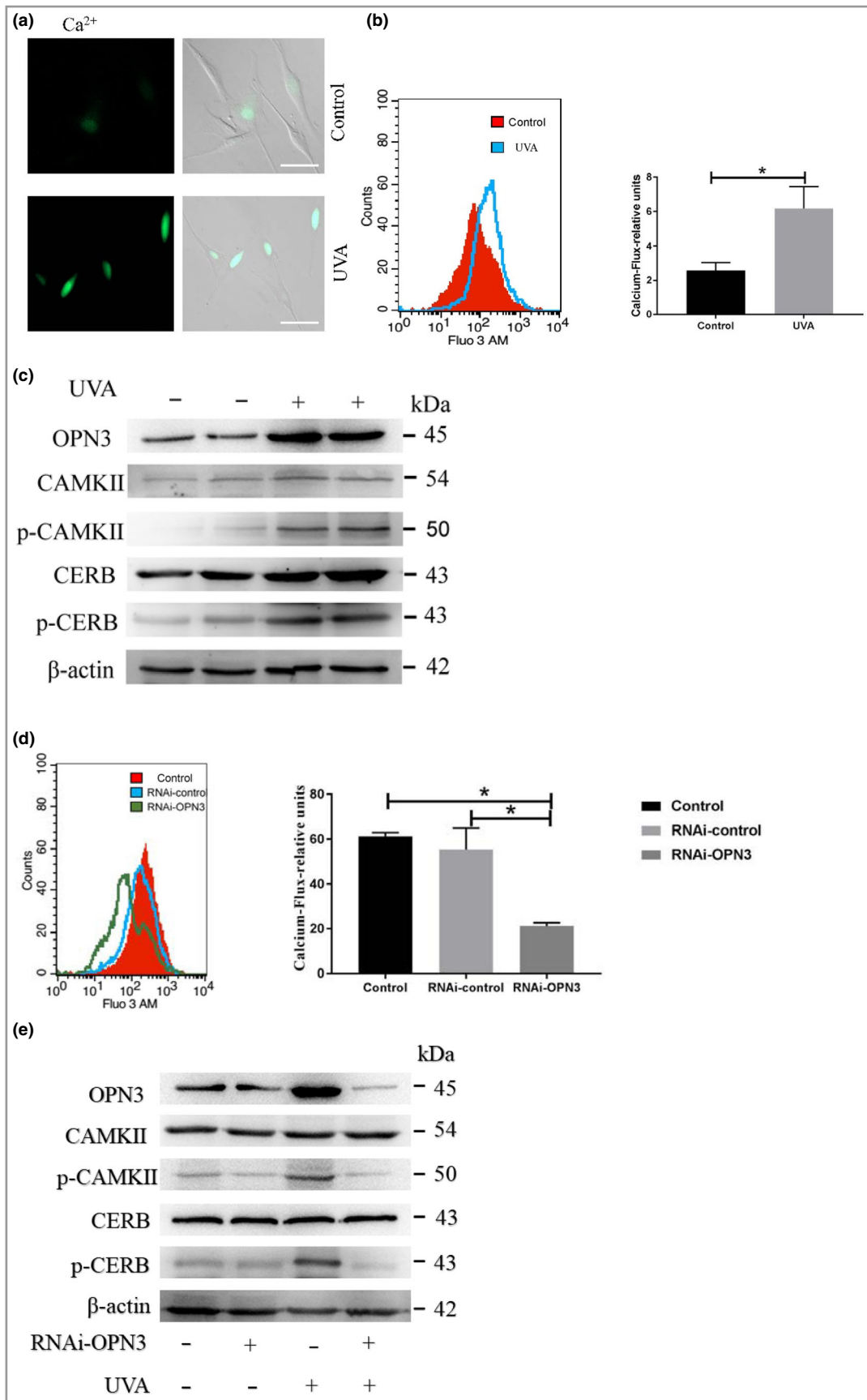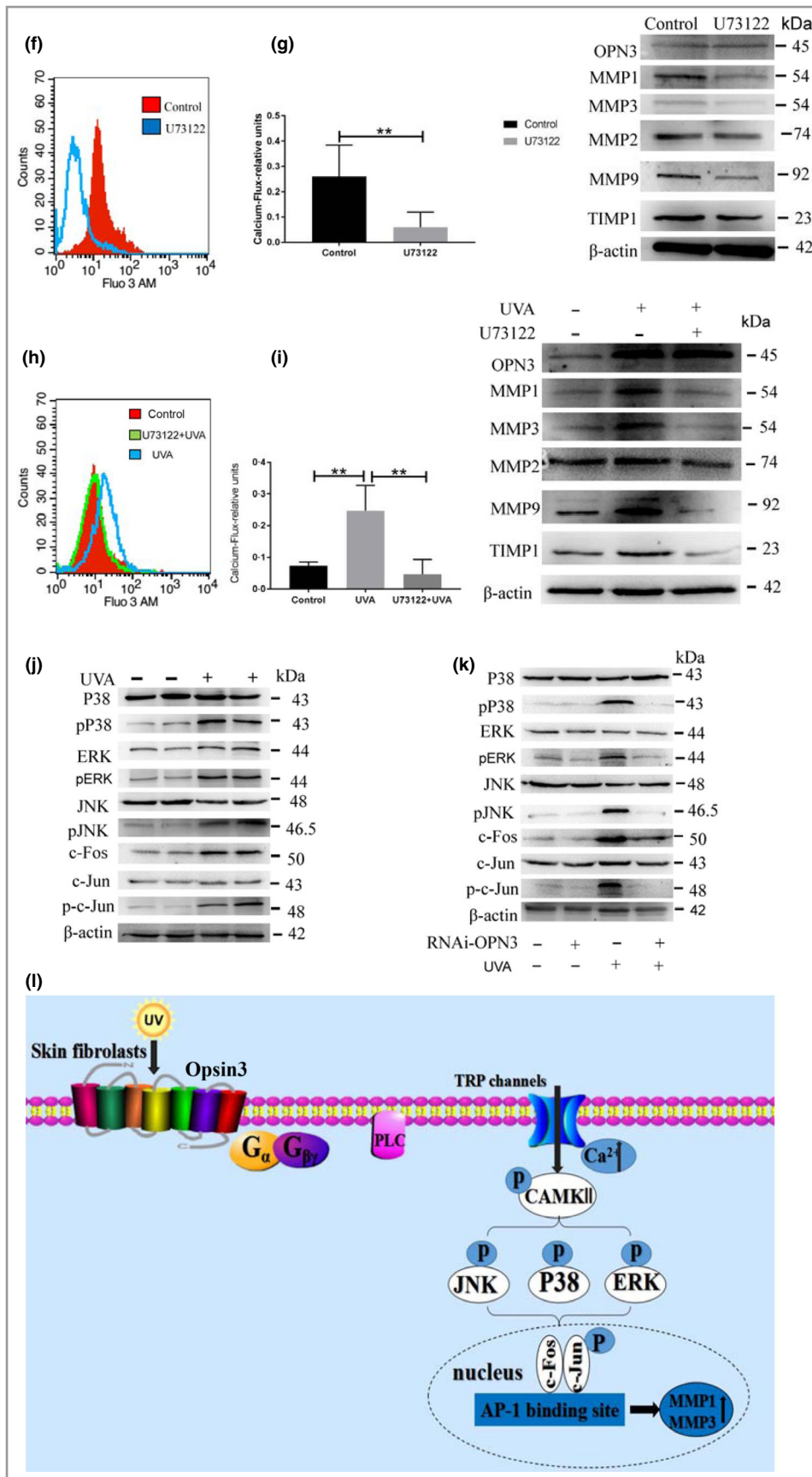
Fig 5. Continued.

in a dose-dependent manner in NHDFs (Fig. 2a). Studies indicate that the absorption spectrum of OPN3 may be wider and we found that OPN1, OPN3 and OPN5 respond to UVA exposure. In particular, the response of OPN3 to UVA was significantly higher than that of OPN1 and OPN5. Moreover, our previous studies found that when siRNA was used to inhibit OPN3, the expression of other OPNs was also downregulated. It is possible that OPN3 plays an important role in cells and forms a complex with other OPNs to regulate OPN expression. More experimental data is required to investigate this hypothesis further. Surprisingly, OPN3 is involved in the upregulation of MMP1, MMP2, MMP3, MMP9 and TIMP1 in NHDFs. These findings suggest that OPN3 plays an important role in fibroblasts. We sought to elucidate the physiological roles and signalling pathways of OPN3, a nonocular OPN, in NHDFs.

It is well known that long-wave UVA is the major environmental factor that causes skin photoageing, which is characterized by prominent alterations in the collagenous extracellular matrix of connective tissue in the dermis,[4,5] and overexpression of MMP1, MMP2, MMP3 and MMP9 in dermal fibroblast cells is the key pathological basis of the photoageing process.[49,50] High expression of MMP1, MMP2, MMP3 and MMP9 was also confirmed in our photoageing model (Fig. 3c). However, it is unclear how human skin senses and responds to UVA irradiation and subsequently induces downstream signalling cascades. An understanding of photochemistry is based on the Grotthuss–Draper law, which states that photon energy must be absorbed in order to have a subsequent reaction.[51] In order to understand the mechanisms that drive photoageing of human skin, it is necessary to identify which molecules act as UVR absorbers and where these molecules are located (in cellular or intracellular compartments). Previous studies have suggested that some small molecules may act as UVR chromophores (and in some cases as photosensitizers), including urinary acids, porphyrins and flavins, vitamin K and B6 derivatives, bilirubin, nicotinamide adenine dinucleotide phosphate and advanced glycation end products.[4] However, it is still unclear which key protein molecules are responsible for absorbing photons. In this study, we demonstrate that the effect of UVA on the upregulation of the expression of MMP1, MMP2, MMP3 and MMP9 in fibroblasts is mediated by OPN3. UVA acts directly on NHDFs to upregulate the expression of MMP1, MMP2, MMP3 and MMP9 (Fig. 4d, e) and in this process OPN3 serves as the sensor for UVA in NHDFs. When the OPN3 gene was silenced, UVA could no longer upregulate expression of MMP1, MMP2, MMP3 and MMP9 (Fig. 4d, e).

We then studied the signalling pathway leading to this OPN3-mediated phenomenon. Previous studies have reported that GPCR drives calcium mobilization in intracellular storage in melanocytes,[19,20] and participates in the downstream signal cascade reaction. To assess the contribution of extracellular and intracellular Ca^{2+} to this signalling pathway, we measured the response of UVA-induced NHDFs in Ca^{2+}-free extracellular buffer and found a significant increase in intracellular Ca^{2+} (Fig. 5a, b). Meanwhile, UVA induced the upregulation of p-

CAMKII, which is a key enzyme in the calcium pathway (Fig. 5c), suggesting that in NHDFs, UVA exposure induces Ca^{2+} mobilization from intracellular stores. Previous studies have shown that CREB phosphorylation plays a role in mediating CREB activation downstream of cyclic adenosine monophosphate[52,53] and CREB is a primary downstream target of CAMKII.[36,37,53] In this study, we show that CAMK activation leads to phosphorylation of CREB (Fig. 5c). Next, to test whether Ca^{2+} mobilization is initiated downstream of GPCR activation, we measured the UVA-induced response in NHDF knockdown OPN3 with siRNA and found that preincubation significantly reduced Ca^{2+} response (Fig. 5d) and the protein level of pCAMKII and pCREB was not altered (Fig. 5e). As G protein can cause Ca^{2+} release by phospholipase Cβ PLCβ activation,[19] we tested the effect of PLC antagonist U73122 on UVA-induced Ca^{2+} responses. The data in Figure 5h showed that U73122 significantly inhibited UVA-induced Ca^{2+} transients, with no significant change in the level of MMP1, MMP2, MMP3 and MMP9 protein expression (Fig. 5i). Previous studies have reported that UV-induced reactive oxygen species (ROS) upregulate the expression of MMPs via the MAPK/AP-1 signalling pathway.[5,51] However, recent studies have reported that UVB-induced ROS or calcium signalling upregulate the expression of MMPs via the MAPK/AP-1 signalling pathway in HS68 cells.[54] Alterations in Ca^{2+} levels are important in cell signalling.[55,56] Interestingly, in our study when blocking calcium influx, we found that the MAPK/AP-1 signalling pathway was unresponsive and that the protein expression levels of MMP1, MMP2, MMP3 and MMP9 were not significantly changed (Fig. 5). These results demonstrate that UVA upregulates the expression of MMP1, MMP2, MMP3 and MMP9 through OPN3, which is calcium dependent (Fig. 5l).

In summary, our study demonstrates for the first time the expression of OPN on human dermal fibroblast membranes. In response to UVA irradiation, OPN3 relies on the calcium pathway to activate and upregulate MMP expression, and thus acts as a photoreceptor that plays an important role in photoageing of the skin.

References

1 Muñoz MJ, Nieto Moreno N, Giono LE *et al.* Major roles for pyrimidine dimers, nucleotide excision repair, and ATR in the alternative splicing response to UV irradiation. *Cell Rep* 2017; **18**:2868–79.

2 Rezzani R, Rodella LF, Favero G *et al.* Attenuation of ultraviolet A-induced alterations in NIH3T3 dermal fibroblasts by melatonin. *Br J Dermatol* 2014; **170**:382–91.

3 Fisher GJ, Wang ZQ, Datta SC *et al.* Pathophysiology of premature skin aging induced by ultraviolet light. *N Engl J Med* 1997; **337**:1419–28.

4 Watson RE, Gibbs NK, Griffiths CE, Sherratt MJ. Damage to skin extracellular matrix induced by UV exposure. *Antioxid Redox Signal* 2014; **21**:1063–77.

5 Kammeyer A, Luiten RM. Oxidation events and skin aging. *Ageing Res Rev* 2015; **21**:16–29.

6 Quan T, Qin Z, Xia W *et al.* Matrix-degrading metalloproteinases in photoaging. *J Investig Dermatol Symp Proc* 2009; **14**:20–4.

7 Yau KW, Hardie RC. Phototransduction motifs and variations. *Cell* 2009; **139**:246–64.

8 Smith SO. Structure and activation of the visual pigment rhodopsin. *Annu Rev Biophys* 2010; **39**:309–28.

9 He Y, Gao X, Goswami D *et al.* Molecular assembly of rhodopsin with G protein-coupled receptor kinases. *Cell Res* 2017; **27**:728–47.

10 Sagoo MS, Lagnado L. G-protein deactivation is rate-limiting for shut-off of the phototransduction cascade. *Nature* 1997; **389**:392–5.

11 Terakita A. The opsins. *Genome Biol* 2005; **6**:213.

12 Audet M, Bouvier M. Restructuring G-protein- coupled receptor activation. *Cell* 2012; **151**:14–23.

13 Campbell AP, Smrcka AV. Targeting G protein-coupled receptor signalling by blocking G proteins. *Nat Rev Drug Discov* 2016; **17**:789–803.

14 Sawant OB, Horton AM, Zucaro OF *et al.* The circadian clock gene Bmal1 controls thyroid hormone-mediated spectral identity and cone photoreceptor function. *Cell Rep* 2017; **21**:692–706.

15 Pennisi E. Opsins: not just for eyes. *Science* 2013; **339**:754–5.

16 Haltaufderhyde K, Ozdeslik RN, Wicks NL *et al.* Opsin expression in human epidermal skin. *Photochem Photobiol* 2015; **91**:117–23.

17 Wang Y, Lu H. Opsin expression in human epidermis melanocytes co-cultured with keratinocytes *in vitro. J Invest Dermatol* 2017; **137** (Suppl. 1):S127.

18 Leung NY, Montell C. Unconventional roles of opsins. *Annu Rev Cell Dev Biol* 2017; **33**:241–64.

19 Wicks NL, Chan JW, Najera JA *et al.* UVA phototransduction drives early melanin synthesis in human melanocytes. *Curr Biol* 2011; **21**:1906–11.

20 Regazzetti C, Sormani L, Debayle D *et al.* Melanocytes sense blue light and regulate pigmentation through opsin-3. *J Invest Dermatol* 2018; **138**:171–8.

21 Castellano-Pellicena I, Uzunbajakava NE, Mignon C *et al.* Does blue light restore human epidermal barrier function via activation of Opsin during cutaneous wound healing? *Lasers Surg Med* 2019; **51**:370–82.

22 Tsukamoto H, Chen IS, Kubo Y, Furutani Y. A ciliary opsin in the brain of a marine annelid zooplankton is ultraviolet-sensitive, and the sensitivity is tuned by a single amino acid residue. *J Biol Chem* 2017; **292**:12971–80.

23 Sikka G, Hussmann GP, Pandey D *et al.* Melanopsin mediates light-dependent relaxation in blood vessels. *Proc Natl Acad Sci USA* 2014; **111**:17977–82.

24 Kojima D, Mori S, Torii M *et al.* UV-sensitive photoreceptor protein OPN5 in humans and mice. *PLOS ONE* 2011; **6**:e26388.

25 Mure LS, Hatori M, Ruda K *et al.* Sustained melanopsin photoresponse is supported by specific roles of β-Arrestin1 and 2 in deactivation and regeneration of photopigment. *Cell Rep* 2018; **25**:2497–509.e4.

26 Fernald RD. Casting a genetic light on the evolution of eyes. *Science* 2006; **313**:1914–18.

27 Ozdeslik RN, Olinski LE, Trieu MM *et al.* Human nonvisual opsin 3 regulates pigmentation of epidermal melanocytes through functional interaction with melanocortin 1 receptor. *Proc Natl Acad Sci USA* 2019; **116**:11508–17.

28 Lee YK, Cha HJ, Hong M *et al.* Role of NF-κB-p53 crosstalk in ultraviolet A-induced cell death and G1 arrest in human dermal fibroblasts. *Arch Dermatol Res* 2012; **304**:73–9.

29 Xu X, Zheng Y, Huang Y *et al.* Cathepsin D contributes to the accumulation of advanced glycation end products during photoaging. *J Dermatol Sci* 2018; **90**:263–75.

30 Huang Y, Li Y, Hu Z *et al.* Mimicking melanosomes: polydopamine nanoparticles as artificial microparasols. *ACS Cent Sci* 2017; **3**:564–9.

31 Ocampo A, Reddy P, Martinez-Redondo P *et al.* In vivo amelioration of age-associated hallmarks by partial reprogramming. *Cell* 2016; **167**:1719–33.e12.

32 Debacq-Chainiaux F, Erusalimsky JD, Campisi J, Toussaint O. Protocols to detect senescence-associated beta-galactosidase (SA-beta-gal) activity, a biomarker of senescent cells in culture and *in vivo. Nat Protoc* 2009; **4**:1798–806.

33 Li Y, Zhao H, Huang X *et al.* Embryonic senescent cells re-enter cell cycle and contribute to tissues after birth. *Cell Res* 2018; **28**:775–8.

34 Min W, Liu X, Qian Q *et al.* The effects of baicalin against UVA-induced photoaging in skin fibroblasts. *Am J Chin Med* 2014; **42**:709–27.

35 Dolmetsch R. Excitation-transcription coupling: signaling by ion channels to the nucleus. *Sci STKE* 2003; **2003**:PE4.

36 Sato K, Suematsu A, Nakashima T *et al.* Regulation of osteoclast differentiation and function by the CaMK-CREB pathway. *Nat Med* 2006; **12**:1410–16.

37 Ma H, Groth RD, Cohen SM *et al.* γCaMKII shuttles Ca2+/CaM to the nucleus to trigger CREB phosphorylation and gene expression. *Cell* 2014; **159**:281–94.

38 Ernst OP, Lodowski DT, Elstner M *et al.* Microbial and animal rhodopsins: structures, functions, and molecular mechanisms. *Chem Rev* 2014; **114**:126–63.

39 Lamb TD, Collin SP, Pugh EN Jr. Evolution of the vertebrate eye: opsins, photoreceptors, retina and eye cup. *Nat Rev Neurosci* 2007; **8**:960–76.

40 Pérez JH, Tolla E, Dunn IC *et al.* A comparative perspective on extra-retinal photoreception. *Trends Endocrinol Metab* 2019; **30**:39–53.

41 de Assis LVM, Moraes MN, Magalhães-Marques KK, Castrucci AML. Melanopsin and rhodopsin mediate UVA-induced immediate pigment darkening: unravelling the photosensitive system of the skin. *Eur J Cell Biol* 2018; **97**:150–62.

42 Toh PP, Bigliardi-Qi M, Yap AM *et al.* Expression of peropsin in human skin is related to phototransduction of violet light in keratinocytes. *Exp Dermatol* 2016; **25**:1002–5.

43 Lan Y, Lu H. Opsin expression in human dermis fibroblasts *in vitro. J Invest Dermatol* 2018; **138** (Suppl.):S189.

44 de Assis LVM, Moraes MN, Castrucci AML. Heat shock antagonizes UVA-induced responses in murine melanocytes and melanoma cells: an unexpected interaction. *Photochem Photobiol Sci* 2017; **16**:633–48.

45 Buscone S, Mardaryev AN, Raafs B *et al.* A new path in defining light parameters for hair growth: discovery and modulation of photoreceptors in human hair follicle. *Lasers Surg Med* 2017; **49**:705–18.

46 Halford S, Freedman MS, Bellingham J *et al.* Characterization of a novel human opsin gene with wide tissue expression and identification of embedded and flanking genes on chromosome 1q43. *Genomics* 2001; **72**:203–8.

47 Koyanagi M, Takada E, Nagata T *et al.* Homologs of vertebrate Opn3 potentially serve as a light sensor in non-photoreceptive tissue. *Proc Natl Acad Sci USA* 2013; **110**:4998–5003.

48 Arendt D, Tessmar-Raible K, Snyman H *et al.* Ciliary photoreceptors with a vertebrate-type opsin in an invertebrate brain. *Science* 2004; **306**:869–71.

49 Scharffetter-Kochanek K, Brenneisen P, Wenk J *et al.* Photoaging of the skin from phenotype to mechanisms. *Exp Gerontol* 2000; **35**:307–16.

50 Naru E, Suzuki T, Moriyama M *et al.* Functional changes induced by chronic UVA irradiation to cultured human dermal fibroblasts. *Br J Dermatol* 2005; **153**:6–12.

51 Wondrak GT, Jacobson MK, Jacobson EL. Endogenous UVA-photo-sensitizers: mediators of skin photodamage and novel targets for skin photoprotection. *Photochem Photobiol Sci* 2006; **5**:215–37.

52 Naqvi S, Martin KJ, Arthur JS. CREB phosphorylation at Ser133 regulates transcription via distinct mechanisms downstream of cAMP and MAPK signalling. *Biochem J* 2014; **458**:469–79.

53 Dolmetsch RE, Pajvani U, Fife K *et al.* Signaling to the nucleus by an L-type calcium channel-calmodulin complex through the MAP kinase pathway. *Science* 2001; **294**:333–9.

54 Hwang YP, Kim HG, Han EH *et al.* N-Acetylglucosamine suppress collagenases activation in ultraviolet B-irradiated human dermal fibroblasts: involvement of calcium ions and mitogen-activated protein kinases. *J Dermatol Sci* 2011; **63**:93–103.

55 Clapham DE. Calcium signaling. *Cell* 2007; **131**:1047–58.

56 Yano S, Tokumitsu H, Soderling TR. Calcium promotes cell survival through CaM-K kinase activation of the protein-kinase-B pathway. *Nature* 1998; **396**:584–7.

Supporting Information

Additional Supporting Information may be found in the online version of this article at the publisher's website:

Powerpoint S1 Journal Club Slide Set.